10

Characterization of the Firing Steps and Phases Formed in Mg-Zr-Containing Refractory Dolomitic Materials

Araceli Lavat, María Cristina Grasselli and Eugenia Giuliodori Lovecchio
Facultad de Ingeniería, U.N.C.P.B.A.
Argentina

1. Introduction

The production of cement clinker is one of the most important industrial processes at world scale. Many technological innovations have been developed in order to increase the production at a lower cost, having in mind that the materials are exposed to severe operational conditions. The fabrication process of modern Portland clinker basically involves the firing at around 1500°C of limestone-$CaCO_3$ accompanied by silica-SiO_2 sources such as clays, sand, iron ore, shale, fly ashes and slags. The final product is a synthetic mineral called clinker which is basically formed by four crystalline phases: alite (Ca_3SiO_5), belite (β-Ca_2SiO_4), tricalcium aluminate ($Ca_3Al_2O_6$) and ferrite ($Ca_2(Al_xFe_{2-x})_2O_5$); and other minor common components. Therefore the process involves aggressive basic environments and atmospheres, with high alkali and sulphur contents, that can strongly modify the microstructure and phase composition of the refractories of the kilns work zone (Kingery et al., 1976).
On the other hand, over the last decades the substitution of fossil fuels for alternative or industrial wastes; such as rubber, used tires, fly ashes, among others; has affected drastically the useful life and performance of the refractory bricks which coat the rotary kilns. Nowadays the burning zone of the kilns is exposed to alkali salts, chlorine, sulphur oxides, proceeding from industrial by products or hazardous products of animal origin, that enhance the corrosion process of the kilns refractory. This technological problem is the reason for focussing in the development of new suitable refractories. Improvements have been made by using higher purity raw materials; however there are economic limits and therefore other more sustainable alternatives are necessarily searched.
According to the modern tendencies in refractories the improvements in the thermal, chemical and mechanical properties of refractories are related to the optimization of the matrix, through the careful design of the mixture of the phases and the microstructural characteristics. As it is well known the performance of these structural parts is a function of the grain material, the nature of the bonding phase, and the distribution and shape of grains and pores. The increase in the proportion of "direct" bonding between refractory aggregate grains is very important. Furthermore the microstructural bonding is the main attribute for an adequate refractory matrix because it contributes to the resistance by the combination of rigidity and sufficient structural flexibility in order to prevent the formation of cracks and disintegration of the hot phase.

The periclase-MgO has excellent refractory properties due to the high melting point (2800°C), strongly basic, without being toxic and good corrosion resistance. All these characteristics have determined the importance of this material as refractory in the cement industry, during the last 65 years. Notwithstanding its use has been limited in rotary kilns due to low thermal shock resistance (Kingery et al., 1976).

In fired magnesia-based bricks, the low-melting bond phases are silicates which melting ranges are a function of the molar ratio of CaO to SiO_2. Silicate-bonded magnesia chromite contain magnesia (MgO) and chromite ($(Mg,Fe)(Cr,Al)_2O_4$) grains with silicates at the grain boundaries. In this system the "direct" attachment of magnesia to chromite occurs without any interrupting film of silicate. These materials show a high resistance to a wide variety of slag and stability under vacuum at high temperature (Goto&Lee, 1995; Qotaibi et al., 1998). Although magnesia-chrome refractory has excellent thermo-mechanical characteristics, the use of these materials has been restrained in many countries due to environmental considerations and governmental regulations concerning the chrome-wastes that they generate and because of their dangerousness. The environmental protection is due to the carcinogenic issues related to hexavalent chromium (CrO_4^{2-}). In view of these refractories wastes with more than 5 mg/l of Cr are forbidden in Europe and USA (Obregón et al., 2011).

Containing chrome-free materials in clinker kilns has been one of the most important challenges in cement industry. In some years later the addition of $MgAl_2O_4$-spinel to MgO was a possible alternative for refractories with a significant improvement of the thermo-mechanical properties of magnesia material. The spinel mixed oxide is very attractive as refractory material in heavy industries because it exhibits an unusual combination of properties: high melting point (2135°C), low thermal expansion, considerable hardness, high resistance to chemical attack, favourable chemical stability, and good thermal spalling (Domanski et al., 2004). Based on their properties these materials are being used for lining by glass, cement and siderurgy industries.

Magnesia-spinel refractories are usually prepared by sintering from high alumina cement and synthetic $MgAl_2O_4$-spinel. However, at present, the cost of the sintered and electrofused spinels has limited their applications. Consequently, in view of the irreplaceable character of such materials in the industry, alternative routes focused on the synthesis of this kind of refractories, by a more economic procedure, have been developed. In this way the preparation of calcium aluminate cements containing $MgAl_2O_4$-spinel using appropriate mixtures of active alumina and dolomite from Spain and Egypt has been reported (De Aza et al., 2003; Khalil et al., 2001). On the other hand, it has been described, recently, a similar way of synthesis using a dolomitic raw material from Argentine, and the α and γ polymorphs of alumina, commercially available. (Lavat & Grasselli, 2007; Lavat et al., 2009). According to these results, independently of the type of alumina used, a mixed phase product consisting of spinel, as a major phase, accompanied by $CaAl_2O_4$ (CA) and $CaAl_4O_7$ (CA_2), as secondary phases, was obtained. In addition, it was found that the formation of spinel phase at lower temperature is favoured by γ-Al_2O_3.

Although these materials are conventionally applied refractories, their composition is not adequate, from the thermodynamic point of view, as they would form liquids at low temperature (≈1400°C) when combined with the components of cement, as can be recognized from the phase equilibrium diagram in the system Al_2O_3-CaO-MgO-SiO_2 (Obregón et al., 2011). Furthermore, magnesia-spinel refractories present relatively low

corrosion resistance under the work conditions in the cement kilns, developing hot points. In the beginning of the corrosion process the liquid phase of clinker penetrates inside the substrates through open porosity and grain boundaries.

It is in this context that, in recent years, the calcium zirconate ($CaZrO_3$)-magnesium oxide (MgO) composite material is an interesting alternative for replacing the $MgAl_2O_4$-MgO system, which has become important for the development of cement industry, due to their enhanced refractoriness (Contreras et al., 2005). On the other hand $CaZrO_3$-MgO is relevant, from the environmental point of view, because it is an ecological alternative for the development of cement industry, due to the fact that non dangerous wastes are generated. In particular $CaZrO_3$ is a phase of high melting point (≈2340°C), without polymorphic transformations, which is compatible with MgO and Portland cement silicates, very resistant to the penetration of fluxes from the clinker (Obregón et al., 2011).

In this system, a so-called elastic direct bond between MgO and $CaZrO_3$ has been reported. Due to this bonding formation and the high refractoriness of $CaZrO_3$, the MgO-$CaZrO_3$ composite materials are characterized by a high hot mechanical resistance and an excellent corrosion resistance against alkaline, earth alkaline oxides and basic slag (Serena et al., 2004). Moreover from the analysis of the *post-mortem* bricks conformed from the above mentioned materials, it was demonstrated a higher corrosion resistance than in MgO-chrome or MgO-spinel refractories (Rodríguez-Galicia et al., 2007).

On the other hand, MgO-$CaZrO_3$ composite refractories also can be synthesized from low cost raw materials, as dolomite, by mixing this mineral with the adequate stoichiometric amount of commercial zirconium sources, using a conventional solid-state reaction (Serena et al., 2005; Suzuki et al., 2000). Dolomite ores are available around the world and Zr occurs widely over the earth crust, but not in very concentrated deposits; as the major minerals are baddeleyite-ZrO_2 and zircon- $ZrSiO_4$. Undoubtedly, this seems an attractive route for the production at low cost of the Mg-Zr-based high temperature structural material.

Considering that the most important dolomite mineral resources in Argentine are located in Olavarría District, close to cement plants, and in order to advance in the feasibility of application of these potentially useful raw materials, our investigation has been extended to the preparation of MgO-$CaZrO_3$ refractories for the cement industry.

In order to establish the most adequate synthesis condition for the composite refractory materials, two batches, containing commercial grade zirconia-ZrO_2 and zircon-$ZrSiO_4$, labeled D-Z and D-ZS, respectively, with the appropriate amount of the dolomitic ore (D), were prepared. The thermal and structural changes which take place during the firing of the batches up to 1400°C were studied by the combination of diffractometric and infrared spectroscopy data, at the most remarkable reaction steps. The microstructures of the final products of each specimen were also analyzed.

2. Experimental procedure

2.1 Materials characterization

The starting materials employed in this investigation were a commercially available zirconia (CF-Plus, Z-Tech) and industrial grade zircon (Kreutzonit), which were mixed with the adequate molar ratio of a dolomitic mineral ore supplied by Polysan S.A. Company (Polysan M. R., Sierras Bayas, Bs. As., Argentine). A sieved dolomite fraction ≤125μm was characterized from its chemical, mineralogical and grain size properties.

The chemical composition was determined by X-ray fluorescence wavelength dispersive technique. The automatic fusion with lithium tetraborate was applied as preparation sample method. Reference certificated materials were used for calibration.
The particle size analysis was determined by laser granulometry, in wet suspensions with isopropylic alcohol, using a Malbern-Mastersizer-S apparatus. The chemical composition, mean particle size "d" and specific surface area "S" results of samples are given in Table 1.

Composition	**Raw Materials**		
	Zirconia	**Zircon**	**Dolomite**
SiO_2	0,90	33	6,56
ZrO_2	96,7	64	-
Al_2O_3	0,20	-	1,47
Fe_2O_3	0,05	<0,10	1,63
TiO_2	0,10	<0,15	0,11
P_2O_5	-	-	0,03
MnO	-	-	0,08
CaO	0,05	-	29,60
MgO	0,01	-	17,83
Na_2O	0,05	-	<0,01
K_2O	-	-	0,43
SO_3	-	-	<0,01
HfO_2	1,90	2,5	-
Y_2O_3	0,15	-	-
U	0,025	-	-
Th	0,01	-	-
L.O.I. 1000 °C	-	-	42,07
d (μm)	13,00	1,61	24,27
S (m2/g)	31,7	11,1	2,4
L.O.I.: Loss on ignition			

Table 1. Chemical composition (in oxides, wt %. L.I., loss on ignition) and textural properties

The surface area was determined by the BET method through the N_2 adsorption technique at 77 K, using a Quantachrome Nova 1200e pore size and surface area analyzer.
Finely ground polycrystalline samples were mineralogical analysed by FTIR vibracional spectroscopy and X-ray diffraction. The XRD measurements were carried out with an automated PW model 3710 Philips diffractometer, with graphite monochromated Cu Kα radiation. Phase identification analysis was carried out by comparing the respective powder X-ray diffraction patterns with standard database stated by JCPDF and the bibliography information available in the literature. Table 2 shows the PDF records for every material under study together with the formula, name, symbol and main reflections used in this work.

PDF N°	Formula, name	Symbol	d (Å)
36-0426	$CaMg(CO_3)_2$, Dolomite	D	2,8880
05-0586	$CaCO_3$, Calcite	C	3,0350
33-1161	SiO_2, Quartz	Q	3,3420
37-1484	ZrO_2, Monoclinic Zirconia	m-Z, m- ZrO_2	3,1640
34-0104	HfO_2, Hafnium oxide	m-HfO_2	3,1470
37-1497	CaO, Lime	CaO	2,4058
44-1481	$Ca(OH)_2$, Portlandite	CH	2,6270
04-0829	MgO, Periclase	M	2,1060
35-0790	$CaZrO_3$, Calcium zirconate	CZ	2,8340
36-1473	$CaHfO_3$, Ca, Hf oxide	CHf	2,8230
26-0341	$(Zr,Ca)O_2$(ss), (ss:solid solution) stabilized zirconia	Z*	2,9610
21-1152	$MgAl_2O_4$, Spinel	E	2,4370
33-0302	Ca_2SiO_4, Larnite	β-C_2S	2,7830
06-0266	$ZrSiO_4$, Zircon	ZS	3,3020
42-1164	ZrO_2, Tetragonal Zirconia	t-Z, t- ZrO_2	2,9950
31-0298	Ca_2SiO_4, Calcium silicate	CS	2,7960
35-0591	$Ca_3Mg(SiO_4)_2$; Ca,Mg Silicate	CMS	2,6865
41-0185	$Mg_2Zr_5O_{12}$; Zr,Mg oxide	MZO	1,7850

Table 2. Nomenclature, PDF No. and principal diffraction lines of the phases under analysis

The FTIR spectra were measured using a Nicolet-Magna 550 FTIR instrument, with CsI optics applying the KBr "pellets" technique and software OMNIC 3.1. Spectra interpretation was based on published data and FTIR spectra of Minerals Library Software.
The microstructure of the materials was obtained by scanning electron microscopy (SEM) using a Microscope Jeol JSM-6460LV. The X-ray microanalysis was performed by an EDAX Genesis XM4 - Sys 60, equipped with an EDAX mod EDAM IV multichannel analyzer, with Zaffire Si(Li) detector and a ultra thin Be window and software EDAX Genesis versión 5.11

2.2 Samples preparation

Two batches of refractories, labelled D-Z and D-ZS; as already stated, were synthesized in view of the respective phase diagram. Firstly considering the ZrO_2-MgO-CaO ternary system phase diagram (Serena et al., 2005), as well as the chemical composition of raw materials detailed in Table 1, equimolar mixtures of dolomite and zirconia were prepared in order to obtain the refractory material of nominal composition MgO-$CaZrO_3$. After that, according to the ZrO_2-MgO-CaO-SiO_2 quaternary system phase diagram (Rodríguez-Galicia et al., 2005), a mixture containing 78% dolomite with industrial zircon was also manufactured.
The mixtures were dry-homogenized. Half of them were submitted to conventional ceramic procedure by solid state reaction at high temperatures with intermediate grindings. The rest

was pressed at approximately 200 MPa and the "pellets" were thermally treated simultaneously with the powdered sample preparation. Although both alternatives were carried out for purposes of comparison, the latter procedure is more feasible at an industrial level. Firing was carried out in a muffle furnace under atmospheric condition.
To stabilize the ceramic bond, the materials were kept at intermediate temperatures for 1 hour and at the highest temperature for several hours. The samples treated at the various temperatures, in the thermal interval, were mineralogical characterized applying the same methodology as described for raw materials. Based on these results, the optimum temperatures for the in-situ generation of phases were established.

3. Results and discussion

3.1 Raw materials characterization

According to the chemical analysis of raw materials given on Table 1, it may be seen that the major impurities of the dolomitic source under study are SiO_2, Fe_2O_3 and K_2O, bearing a higher SiO_2 content than those used by other researchers which are around 0,02-0,5 weight % (De Aza et al., 2003; Khalil et al., 2001). The presence of these impurities is related to the geological origin of $CaMg(CO_3)_2$ ores. The most important dolomite mineral resources in Argentine, comprises an igneous-metamorphic basement covered by Neoproterozoic sedimentary rocks. These dolostones are characterized by abundant dolomite and low proportions of calcite. Quartz, illite and feldspar are the most common impurities of carbonates fraction. Calcite cements are included in voids and veins and quartz generally is present as silt-sized clasts dispersed in the dolomite matrix, as well as multi-generational cement inside voids. Occasionally silica is present as fine chert (amorphous silica), which fills voids or replaces carbonate. The mineralogical composition estimated by XRD is: dolomite 75-95%, calcite 1–5%, quartz and chert 1–15%, clay minerals <2% and feldspar <1% (Gómez Peral, 2007).
The weight loss of around 40% is compatible with the release of gaseous CO_2. Meanwhile, the mean size particle of the dolomitic mineral, measured by laser granulometry, is 24,27 μm and the surface area is 2,4 m^2/g.
On the other hand, the chemical composition of Zr-sources was also analyzed. In the case of zirconia, the main impurity HfO_2 is normally present in this mineral due to the extremely difficult separation of Zr from Hf. The reason for this is the similarity between the crystal chemistry of Zr(IV) and Hf(IV) which ionic radios are identical. In the light of the chemical similarity between Zr and Hf which is well exemplified in their geochemistry, for Hf is found in nature in all zirconium minerals in the range of a fraction of a percentage of the Zr content (Cotton & Wilkinson, 1988). The amounts of the rest of the elements are negligible. The well-known mechanical and electronic properties of ZrO_2-materials based on total or partially stabilized cubic or tetragonal zirconia have led to their widespread use as structural materials, solid-state electrolytes, catalytic support, and thermal barrier coatings (Serena et al., 2005).
As can be seen, according to the chemical composition, commercial zircon is very pure. The impurities in natural zircon powder limit its applications, especially for high temperature uses (Popa et al., 2006). Notwithstanding the presence of a certain amount of Hf in zircon, as in zirconia, should not be unexpected. $ZrSiO_4$ is commonly used in the pigment industry in the production of glazes and pigments due to their high thermal and chemical stability, as well as for its low thermal expansion coefficient and low thermal conductivity. Zircon sands

are widespread geological occurrence, as a common accessory mineral of igneous rocks and sediments. In technical applications is more advantageous in comparison with ZrO_2 because this oxide is obtained by a complex and expensive process from zircon sands (Ozel & Turan, 2007).

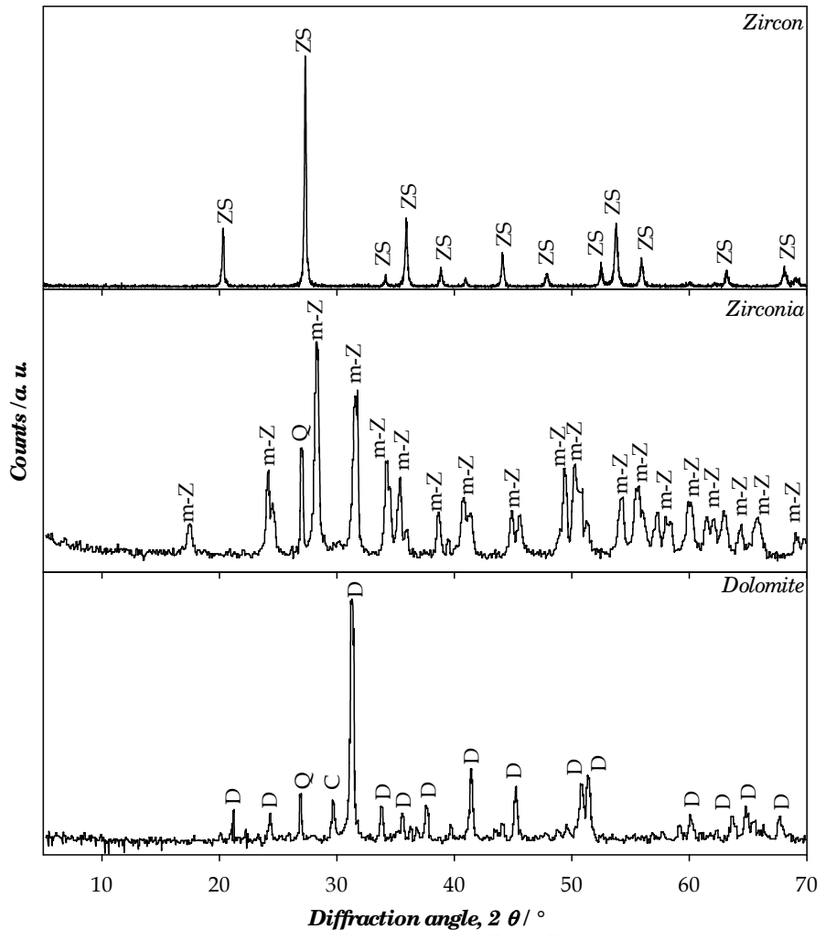

Fig. 1. Minerals characterization of raw materials, XRD patterns

Regarding the particle size and surface properties of both Zr materials, these display lower particle sizes and appreciable higher specific surface than natural dolomite, which should be beneficial for the reactivity of both solids.

In order to analyze the mineralogical composition, the XRD patterns of all the raw materials were registered. The diffractograms are depicted in Fig. 1. In addition, the PDF records for raw materials, as well as the files belonging to the rest of the phases under analysis, are detailed in Table 2, as already stated.

Based on this analysis, it is concluded that the dolomite sample also contains subordinate amounts of calcite (C) and quartz (Q) but in a lesser extent, in accordance with the chemical composition. Quartz is, of course, of almost universal occurrence in dolostones, at least in trace amounts, the enhanced intensity is due to an orientation effect.

In the case of zirconia it is mainly monoclinic zirconium oxide (m-ZrO_2) and presents quartz as impurity. The quartz presence is consistent with the small amount of SiO_2, which was

determined by chemical analysis, in both raw materials, as detailed in Table 1. The presence of HfO_2 could not be determined by DRX because its diffraction pattern is superimposed with the m-ZrO_2 which posses an identical crystal cell.
Regarding the XRD pattern of Zircon, the presence of $ZrSiO_4$ as a pure phase, is confirmed, in accordance with the chemical analysis.
To complete the analysis of the mineral phases present in the raw material the measurement of the vibrational spectra was registered. The FTIR spectral patters are shown in Fig.2.

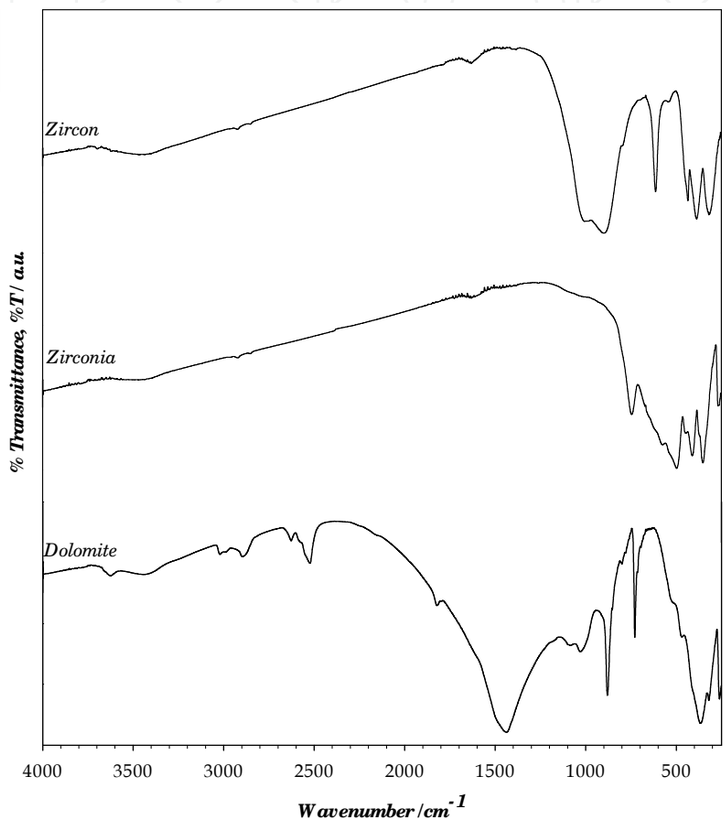

Fig. 2. FTIR of starting materials

Dolomite, which has a calcite-type structure, shows its overall bands among which the diagnostic ones are at 1443, 882 and 728 cm^{-1} belonging to CO_3^{-2} anion, are present, as can be seen in Fig.2. The positions are shifted to higher frequency due to the smaller size of Mg(II) in comparison with Ca(II). Despite the structural differences, calcite bands are not seen because they are located at similar frequencies as dolomite bands (1428, 878 and 714 cm^{-1}) and therefore overlapped with the broad bands of this predominant mineral. Although quartz is a minor constituent, it can clearly be identified by the bands located at 1144 and 1085 cm^{-1}, which are attributed to SiO_4 group vibrations (Wilson, 1987).
The zirconia spectrum, depicted in Fig.2, indicates the presence of isostructural ZrO_2 and HfO_2, both having a monoclinic structure, with contributions to the bands attributed to Zr-O and Hf-O vibrations from the ZrO_7 (HfO_7) units. The six characteristic bands of zirconium oxide can be seen located at: 722, 574, 490, 409, 343 and 258 cm^{-1}. A unique HfO_2 band can be observed at 752 cm^{-1}, the remaining bands (635, 600, 512, 410, 343, 324 and 255 cm^{-1})

belonging to this oxide are hidden behind those of zirconium oxide (Neumayer & Cartier, 2001). These features are in accordance to the low proportion of HfO_2 present in the raw material, as already discussed.

The SiO_4 group vibrations belonging to quartz are observed at 1144 and 1085 cm^{-1}, as in dolomite. However, these are weak; corroborating that amount of quartz present in zirconia is lower than in dolomite, in accordance with the chemical analysis (see Table 1). The additional weak absorptions, centered in 3400 cm^{-1}, 1630 cm^{-1} and 1575 cm^{-1} are assigned to O-H, H-O-H and M-OH (M is Zr or Hf) vibrations respectively, which are attributed to absorbed water to these metal oxides (Neumayer & Cartier, 2001).

Regarding the spectrum of zircon, it may be interpret based on its structure which is formed by chains of alternating edge-sharing SiO_4 tetrahedra and ZrO_8 triangular dodecahedra, running parallel to the c-axis. The spectrum depicted in Fig. 2 exhibit the diagnostic bands of $ZrSiO_4$. The main infrared absorptions observed at 1005 and 900 cm^{-1}, belong to Si-O stretching vibrations, with the deformational mode of SiO_4 unit at 435 and 387 cm^{-1}; the sharp band observed at 613 cm^{-1} are associated to Zr-O bonds of ZrO_8 units (Ozel & Turan, 2007). In addition, the weak absorptions bands located at 3000-2900 cm^{-1} and at 1630 cm^{-1} are due to hydroxyl ion impurities in zircon and deformation of the HOH bonds, respectively (Dawson et al., 1971).

3.2 Evolution of the phases on heating, for D-Z specimens

For the detailed analysis of the phase changes during the preparation of the D-Z refractory, in every thermal step; the relative intensity of the characteristic peaks of each crystalline compound expected to appear was measured, within the temperature range from ambient to 1400ºC. The instrumental conditions were maintained constant in order to obtain the comparison of the same XRD characteristic lines by using "batch program" analysis in PC-APD software (version 3.6). With the same aim a standard procedure was adopted for the preparation of the test specimens as in other related works (Aras, 2004). The typical reflections selected to carry out the analysis are detailed in Table 2. The FTIR spectra measurements were carried out in order to study the structural changes and the formation of the new bonds during the reactions. The microstructure of the final product obtained was evaluated by SEM-EDX analysis.

3.2.1 Evolution of the phases D-Z on heating by X-Ray diffraction

The XRD patterns belonging to the different heating temperatures selected to represent the phase evolution upon calcinations, for the batches labelled D-Z, after heating at 1000, 1150 and 1400°C, are shown in Fig.3.

From X-ray diffraction analysis of the most relevant reaction steps, it was possible to establish that no dolomite is detected after the calcination at 1000°C, in accordance with equation 1, whereas the peak of calcite persists, suggesting that equation 2 has not been completed. At the same time, the main peaks belonging to m-ZrO_2 are still present. The new phases resulting from the thermal decomposition of dolomite and subsequent reaction with zirconia, as $CaZrO_3$ and MgO, were clearly detected, as well as the presence of zirconia, labeled ZrO_2(*ss*), with cubic structure. The typical diffraction lines of both zirconia polymorphs are distinguishable by XRD measurements, accurately, as can be seen from the data available in Table 2. This allows to confirm the formation of a solid solution of $(Zr,Ca)O_2$, commonly called stabilized zirconia, by the solid state reaction between CaO and

m-ZrO_2, with improved mechanical properties. In summary, these results allow affirming that, after the thermal treatment at 1000 °C, the following reactions have occurred:

$$CaMg(CO_3)_2\ (s) \rightarrow CaCO_3\ (s) + MgO\ (s) + CO_2\ (g) \quad (1)$$

$$CaCO_3\ (s) \rightarrow CaO\ (s) + CO_2\ (g) \quad (2)$$

$$CaO\ (s) + \text{m-}ZrO_2 \rightarrow ZrO_2(ss) \quad (3)$$

$$CaO\ (s) + ZrO_2(ss) \rightarrow CaZrO_3\ (s) \quad (4)$$

Despite CaO peaks are absent, giving support to equations 3 and 4, the presence of free lime is discussed later, when FTIR results are analyzed. On the other hand the diffractions belonging to SiO_2, as quartz, accompanying the dolomitic source, remained constant.

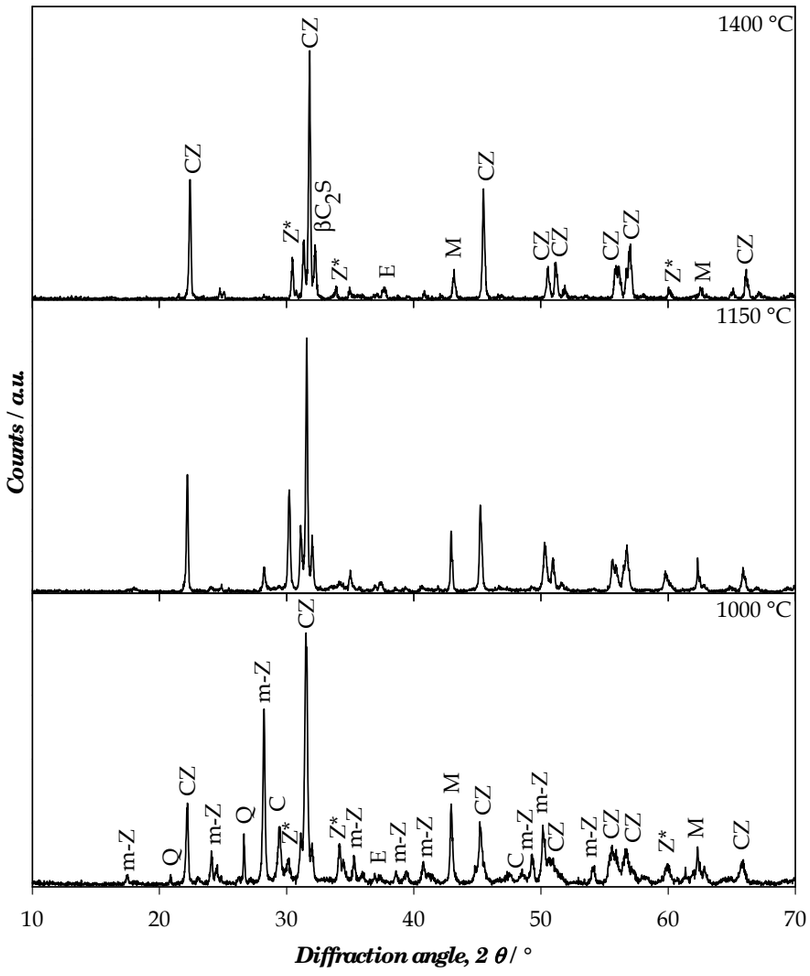

Fig. 3. XRD patterns of sample D-Z, at different firing temperatures

At 1150 °C, the main features observed in the patterns are that the diffraction lines from calcite and quartz disappeared, and instead some new lines belonging to dicalcium silicate,

Ca_2SiO_4, labeled β-C_2S, and the spinel phase $MgAl_2O_4$ appear, at this temperature. The presence of β-C_2S is attributed to the solid state reaction involving SiO_2, from quartz, and CaO available, in accordance with equation 5. The formation of the mixed oxide $MgAl_2O_4$, belonging to the spinel structure, in a minor extent, is supported by the appearance of its main peak as a weak signal. This compound is a consequence of the reaction between free MgO and Al_2O_3 (see equation 6), consistent with the low amount of aluminum oxide, determined by X-ray fluorescence in the raw material (see Table 1). Spinel formation was observed at the same temperature in the previous research, involving the reaction between the dolomitic resource and alumina, in the synthesis of $MgAl_2O_4$-spinel-containing refractory cements (Lavat & Grasselli, 2007; Lavat et al., 2010). Concerning the peaks belonging to m-ZrO_2, these remained but with considerable low intensity. According to these results the following reactions are proposed, after this thermal step:

$$2\ CaO\ (s) + SiO_2\ (s) \rightarrow Ca_2SiO_4\ (s) \quad (5)$$

$$MgO\ (s) + Al_2O_3\ (s) \rightarrow MgAl_2O_4\ (s) \quad (6)$$

When the temperature reaches 1400°C, m-ZrO_2, is not present and simultaneously all the phases formed by the preceding reactions (labeled as CZ, M, ZrO_2 (*ss*), E and β-C_2S in Fig.3), are maintained with increased intensity.

Concerning the presence of a minor amount of HfO_2 in zirconia, the XRD measurements do not recognize the formation of $CaHfO_3$, as the resulting compound from the reaction of available CaO and HfO_2, because the characteristic lines of this solid lay in the same diffraction angle value than the analogous Zr compound, due to the identical crystal sizes. The same consideration has been already reported (Zoz & Karaulov, 1991).

For more detailed information, the XRD main diffraction intensities of every component detected in the patterns is plotted against temperature as depicted in Fig. 4. When there is an overlap of the main peaks for two phases, the second reflection reported in Table 2 was also used. As can be seen in this figure, a sharp decrease is observed in dolomite peaks down to 900°C whereas the rest of the accompanying mineral, as calcite and quartz, as well as zirconia, decline more slowly until around 1100°C and the latter is observable down to 1200°C. These features account for an early temperature of reaction of dolomite and simultaneously the maintenance of zirconia in the original monoclinic structure, in this thermal range.

Regarding the phases formed upon firing, the growth of peak intensities of all the products, $CaZrO_3$, ZrO_2(*ss*), MgO, β-C_2S and $MgAl_2O_4$, is observable over 1100°C. This indicates that the reactions proceed more straightforward over this temperature. Furthermore, as shown in the same figure, a sharp increase is observed in the XRD counts for all components around 1150°C and 1300°C, more markedly in the major components. These features could be attributed to many effects, such as degree of crystallinity, changes in the size of crystals, due to firing, and also with crystal preferential orientation. Nevertheless the general trends of the evolution of the all phases are similar and consequently it may be infer that the rate of formation of the products is similar. A resembling profile has been observed during the preparation of spinel-containing refractory cements, which shows a maximum assignable to the porosity and small grain size of the crystalline phases formed during the reaction (De Aza et al., 2003).

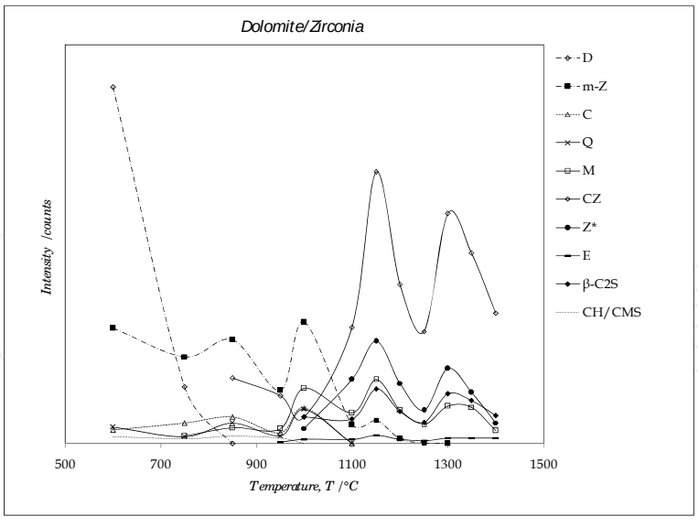

Fig. 4. Evolution of phases during firing for specimen D-Z

The amount of the major phase formed, $CaZrO_3$, (A_{CZ}, in percent), can be estimated from XRD measurements using the following expression, and nomenclature detailed in Table 2:

$$A_{CZ} = [\, I_{CZ} / (I_{CZ} + I_M + I_{Z^*} + I_{\beta\text{-}C2S} + I_E)] \times 100 \quad (7)$$

Where I_i is the integrated intensity of the characteristic diffraction of each phase. A similar methodology was employed in another work (Domanski et al., 2004).

According to this semi-quantitative analysis the proportion of the major phase $CaZrO_3$ in the final mixture, at 1400°C, is 66 %. Whereas the amounts of rest of the components, estimated by the same calculation, are: ZrO_2(*ss*), 10,5%; MgO, 6,6%; β-C_2S, 14% and $MgAl_2O_4$, 2,8%. As can be seen, the amount of β-C_2S is not negligible, in consistence with the relatively high content of SiO_2 found in local dolomite, in comparison with the amount reported for the same mineral in other countries. However the global composition is suitable for refractory purposes. Finally, no vitreous components are observed in the material.

3.2.2 FTIR spectra analysis of specimen D-Z, during firing

The FTIR vibrational spectra depicted in Fig. 5 are suitable to complement XRD information in order to get a more accurate composition of phases at each thermal step during the synthesis of MgO-$CaZrO_3$-containing refractory material. The advantage of using IR spectra is the sensibility and that even amorphous materials can be identified.

According to Fig. 5, after the thermal step at 950°C, the significant bands located at 1443 y 882 cm^{-1} due to the CO_3^{-2} anion, characteristic of dolomite, are observed (Wilson, 1987). It would be necessary to indicate that the characteristic diffraction line of dolomite could not be ascertained by XRD analysis, at this temperature, as already discussed. However, due to the higher sensibility of the spectroscopic technique, these bands are still observed.

In the spectrum of the sample treated 1000°C, the carbonate anion absorptions show a displacement to a lower frequency region, lying at 1428 and 878 cm^{-1}, which are assignable to calcite. Calcite bands are persistent in the spectrum up to 1150°C. These results corroborate the calcite formation at 1000°C, detected from XRD analysis, as a result of the

partial decomposition of dolomite (see equation 1). In addition, according to this technique, the persistence of calcite is ascertained up to 1150ºC.

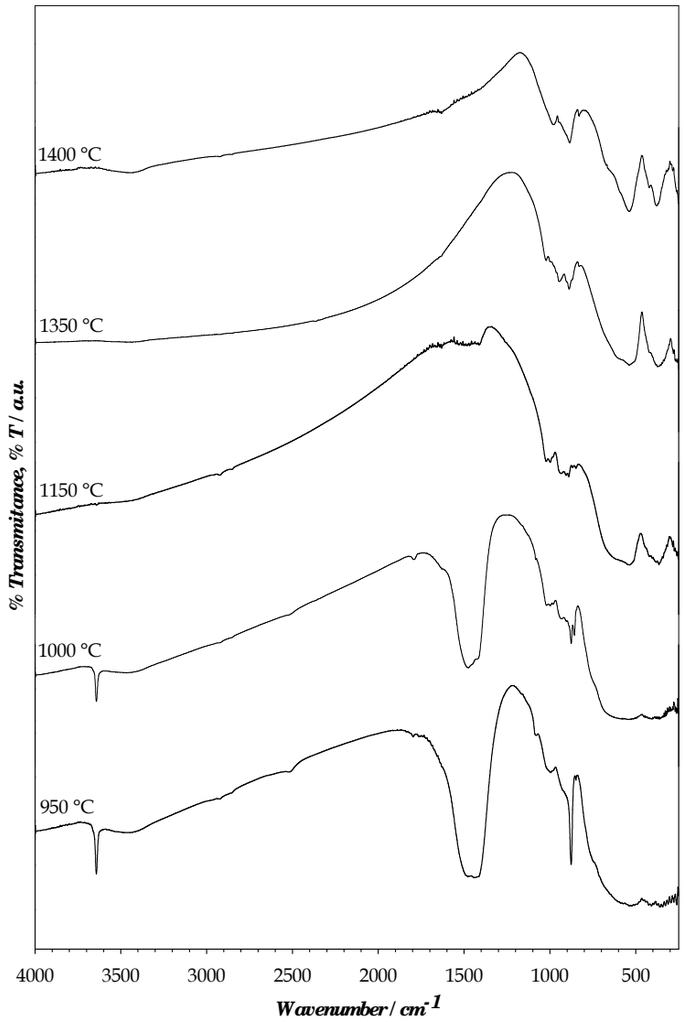

Fig. 5. FTIR spectra of D-Z specimens treated in the thermal range 950-1400 ºC

At the same time, when the spectra of the samples fired over 750°C were analyzed, the presence of portlandite-$Ca(OH)_2$, could be ascertained by the sharp absorption located at 3643 cm^{-1}, assigned to O-H stretching vibration belonging to calcium hydroxide. This band becomes weaker as temperature increases, until it disappears completely at 1000ºC. This spectroscopic evidence is in agreement with the presence of free lime-CaO (see equation 2), since this highly reactive oxide forms portlandite, as a consequence of its ease to react with the atmospheric humidity (Lavat & Grasselli, 2007). However, the characteristic XRD lines belonging to portlandite were not observed due to their superposition with the ones of the other compounds XRD diffractograms, especially with those of zirconia; or furthermore due to the poorly crystallized nature of this solid.

The $CaZrO_3$ is an extremely ionic solid which belongs to the perovskite structure, with orthorhombic symmetry (Orera et al., 1998; Prasanth et al., 2008). The infrared active (IR)

modes are somewhat similar to that of the cubic perovskite. These modes can be described; in decreasing frequency order, as: Stretching of Ca-O (550 cm^{-1}), stretching of Zr-O (400 cm^{-1}) and stretching of Ca-Zr (150 cm^{-1}). Consequently, the signals located at 550 and 400 cm^{-1} which are diagnostic of this phase, are detected from 1100 °C. As the temperature increases these bands become better resolved, in consistence with increasingly calcium zirconate that is formed, as can be seen in the spectrum of the material treated at 1400°C.

This technique neither is suitable to corroborate the formation of $CaHfO_3$, because its bands are located in the same region than the bands associated to $CaZrO_3$. Nevertheless it can be affirmed that HfO_2 has reacted due to the fact that its band located at 752 cm^{-1} has disappeared. For this reason, the formation of $CaHfO_3$ could be supported (Zoz_ & Karaulov, 1991).

Monoclinic ZrO_2 and $CaZrO_3$ phases absorb in the same spectral region due to their similarities in coordination number and bonding characteristics. However, regarding Zr-O vibrations belonging to zirconia, these frequencies are observed at 574 and 490 cm^{-1}, in the spectra of samples treated below to 1350ºC.

The absorptions located between 910-880 cm^{-1} and at 980 cm^{-1}, are attributed to Si-O symmetric and asymmetric stretching, respectively; which are the typical vibrational modes of the silicate moieties forming the structure of the phase β-C_2S (Gou et al., 2005). These bands are observed, in samples submitted to calcination over 1000ºC, and subsequently its definition improves, as a consequence of bond reinforcing with the temperature increases.

The existence of MgO is supported by the presence of a shoulder at 671cm^{-1} in the spectra registered for of all the materials obtained over 750ºC. This frequency is assigned to the stretching of the bonds Mg-O forming the MgO ionic crystal (Singh & Upadhyaya, 1972).

On the other hand, the weak absorptions remaining in the spectrum of the end products calcined at 1400ºC, located at 3400, 1630 and 1575 cm^{-1}, are due to the presence of adsorbed moisture in the samples. In the same way as in zirconia these signals are assigned to O-H, H-O-H, and M-OH vibrations, respectively (Prasanth et al., 2008).

The spectral features of the samples are maintained, showing the maximum definition when the end products are formed, in the final thermal treatment at 1400ºC. Finally, it should be remarked that the FTIR spectra are in full agreement with XRD results. Moreover, the subtle details due to the formation of the new bonds were determined using the spectroscopic tool. Accordingly, the optimal temperature for the refractory material process seems to be 1400ºC.

3.2.3 Microstructure of the material D-Z

In Fig. 6 is presented a SEM micrograph of the bulk porous composite refractory material. The SEM image illustrated in this figure shows a homogenous microstructure consisting of dense rounded borders grains. This morphology should be attributed to the high temperature of synthesis which allows the grain growth and a reduction of porosity. Upon magnification, some degree of inhomogeneity is detected; since over the dark background some clear and smaller particles are observed on the surface. This feature is attributable to the mixed phase system, as determined by the combination of XRD and FTIR measurements.

A careful inspection of the X-ray microanalysis of both regions allows confirming that they differ slightly in the chemical composition. The atomic analysis of the darker particles with block like appearance and some cracks on its surface is composed mainly by Zr and Ca, with a minor amount of Mg and Si, compatible mostly with the presence of $CaZrO_3$, ZrO_2, MgO

and Ca_2SiO_4. On the other hand, in the X-ray microanalysis of the dispersed clear particles, a very low percentage of Al atoms were also identified, it would be attributed to the presence of the spinel $MgAl_2O_4$ phase. Moreover these results are in fair agreement with the global composition estimated from XRD analysis. The elemental compositions measured during the scanning of the surface are similar, suggesting that the components are uniformly distributed in the microstructure.

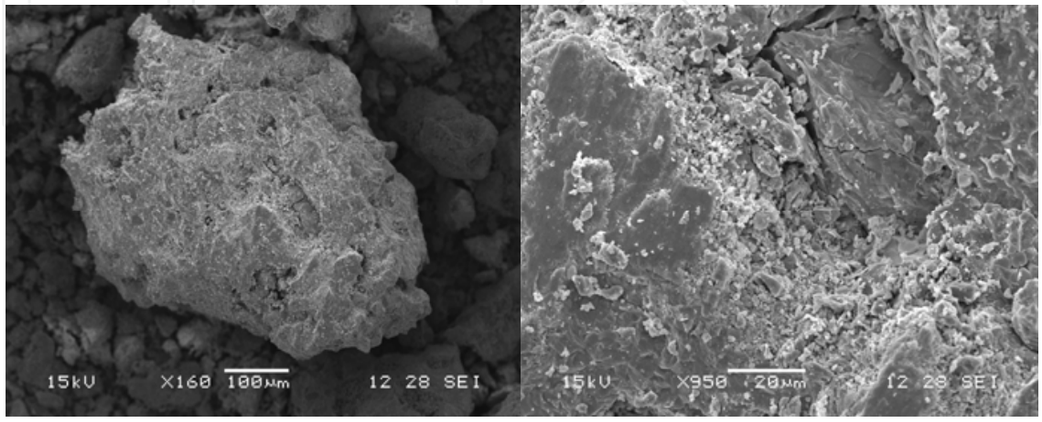

Fig. 6. SEM micrograph of sample D-Z treated at 1400ºC, (left, 160x and right, 950x)

3.3 Formation of refractories from Dolomite-$ZrSiO_3$ mixtures, D-ZS

The behavior of the different batches submitted to firing up to 1350ºC, labelled D-ZS, was evaluated by using the combination of spectroscopic FTIR technique and XRD analysis; using a similar procedure to that described for D-Z specimens. The microstructure of the resulting material was also analyzed.

3.3.1 Evolution of the phases D-ZS on heating by X-Ray diffraction

Some of the XRD patterns belonging to the most relevant heating temperatures are illustrated in Fig. 7. A detailed analysis of the diffractometric results suggests that at 350ºC, only the diffractions belonging to the minerals composing the starting materials, such as dolomite, calcite, quartz and zircon, appear; suggesting that no chemical solid state reactions have occurred yet.

When the batch is submitted to calcination at 850ºC, both carbonate minerals, dolomite and calcite, are no longer observable, whereas quartz and zircon persist. Simultaneously new lines assigned to MgO, t-ZrO_2, ZrO_2(ss), $CaZrO_3$, $Ca_3Mg(SiO_4)_2$ and Ca_2SiO_4, are detected as the result of the apparently complete transformation of the dolomitic raw mineral in the products of the reaction with zircon. The tetragonal polymorph of ZrO_2, which is the thermodynamically stable structure in the phase diagram (Rodríguez et al., 2002) is recognizable. The CaO generated simultaneously, seems to be partly as portlandite-$Ca(OH)_2$ due to its ease to hydration by air moisture. Whereas the remaining CaO, along with some MgO react with zircon and quartz giving rise to $CaZrO_3$, Ca silicate and also the calcium-magnesium silicate already mentioned. A remarkable increase of the characteristic peak of $CaZrO_3$ is observed over 950ºC. In coincidence, the presence of the as called spinel $MgAl_2O_4$ phase is detected (see equation 6). $CaZrO_3$ keep growing to become the major phase at 1050 ºC and at this temperature the apparition of the mixed oxide formulated $Mg_2Zr_5O_{12}$ is

observed. Consequently, these phases seem to be the result of a series of reactions which could be interpreted as follows:

$$3\ CaMg(CO_3)_2\ (s) + 2\ ZrSiO_4\ (s) \rightarrow Ca_3Mg(SiO_4)_2\ (s) + 2\ t\text{-}ZrO_2\ (s) + 2\ MgO\ (s) + 6\ CO_2\ (g) \quad (7)$$

$$CaO\ (s) + t\text{-}ZrO_2\ (s) \rightarrow ZrO_2(ss) \quad (8)$$

$$CaO\ (s) + ZrO_2(ss) \rightarrow CaZrO_3\ (s) \quad (9)$$

$$Ca_3Mg(SiO_4)_2\ (s)\ + CaO\ (s) \rightarrow Ca_2SiO_4\ (s) + MgO \quad (10)$$

$$2\ MgO + 5\ ZrO_2 \rightarrow Mg_2Zr_5O_{12} \quad (11)$$

The peaks of Portlandite, quartz and zircon become not observable at 1000, 1150 and 1200 ^{o}C, respectively; whereas the signal belonging to the t-ZrO_2 polymorph diminishes until disappearance at 1300^{o}C.

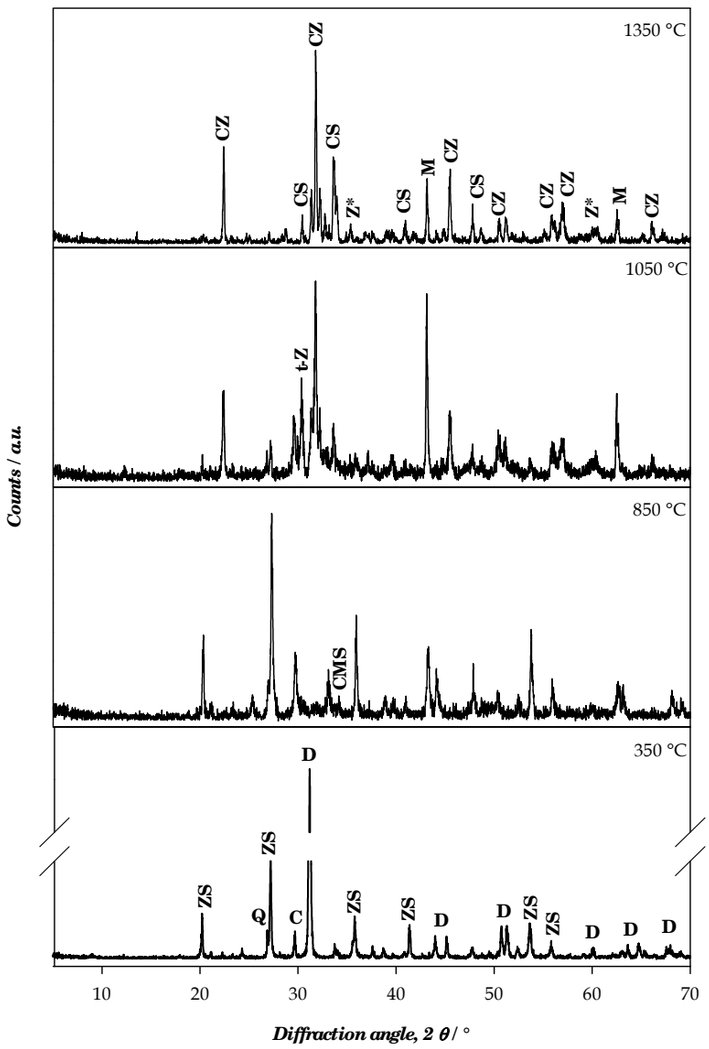

Fig. 7. XRD patterns of sample D-ZS, at different firing temperatures

The compound $Ca_3Mg(SiO_4)_2$ persists until 1050ºC, and then it decomposes upon firing giving rise to Ca_2SiO_4 which is a more stable silicate phase. This result is supported by thermodynamic calculations which establishes a reaction mechanism according to which $Ca_3Mg(SiO_4)_2$ appears as the first phase during the reaction (Rodríguez et al., 2002). It is in this context that the reaction was proposed. Furthermore the coexistence of both silicates, in equilibrium, in the range 850-1100ºC is valid. On the other hand, since this reaction demands CaO to proceed, this suggests that its hydroxide should be present in the mixture ; although it is undetectable by XRD, probably due to superposition with the peaks of other compounds, especially that of calcium silicate, or due to low crystallinity.

The specimen treated at 1350ºC is mainly constituted by $CaZrO_3$, $CaSiO_4$ and MgO. A semi-quantitative XRD analysis of the phases present was carried out by taking into account the peak intensities obtained by XRD data with the appropriate software, as already described.

The amount of the components in the mixed phase is estimated in the proportion 47: 20: 16 %, respectively. The compounds $Mg_2Zr_5O_{12}$, ZrO_2(*ss*) and the so-called spinel phase $MgAl_2O_4$ were detected as minor components. The cubic calcium partially stabilized zirconia is present in the final product, as the result of incorporation of Ca(II) ions to the crystal lattice of t-ZrO_2.

A careful analysis of the evolution of the different phases with the temperature in the range 350-1350ºC, was studied. The peak intensities found for each compound at the main temperatures of synthesis are depicted in Fig. 8.

According to the plotted XRD data of raw minerals, dolomite and calcite show a complete transformation at 850 ºC. Whereas quartz and zircon behave as thermally resistant phases, with a marked decrease over 850 ºC, due to the reaction with the oxides CaO and MgO, released by the dolomitic material, until disappearance around 1150 ºC and 1200ºC, respectively.

In addition to this, the complex interplay of reactions between raw materials and fired products formed during the intermediate steps, justify the trends observed for the phases formed upon calcinations. Nevertheless, the XRD intensities profiles observed suggest that the products formed, $CaZrO_3$, Ca_2SiO_4 and MgO, grow uniformly when the calcination temperature rises. The compounds t-ZrO_2 and $Ca_3Mg(SiO_4)_2$ are transitory phases formed.

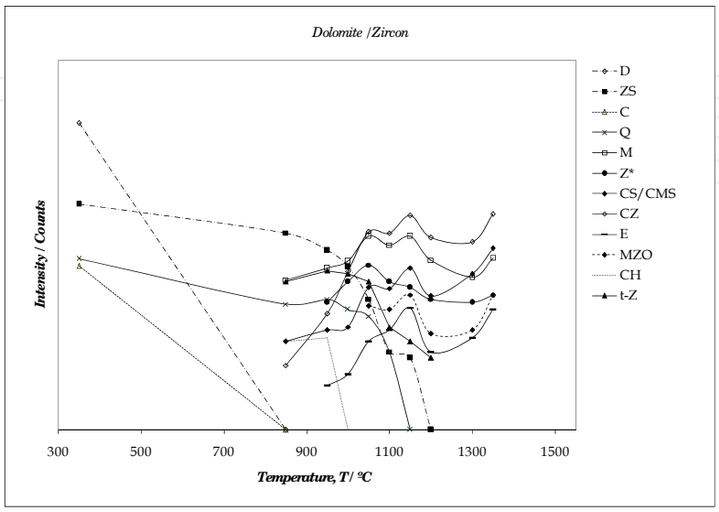

Fig. 8. Evolution of phases, during firing, for D-ZS specimens

3.3.2 FTIR analysis of D-ZS samples, treated in the thermal range 350-1350 ºC

The FTIR spectra of the specimens are in full agreement with the XRD results. In addition, some other evidences, regarding phases not so clearly detected by X-ray diffraction, could be ascertained. The IR data of the calcined samples at different temperatures were analyzed. The spectral patterns of most representative firing steps may be seen in Fig. 9.

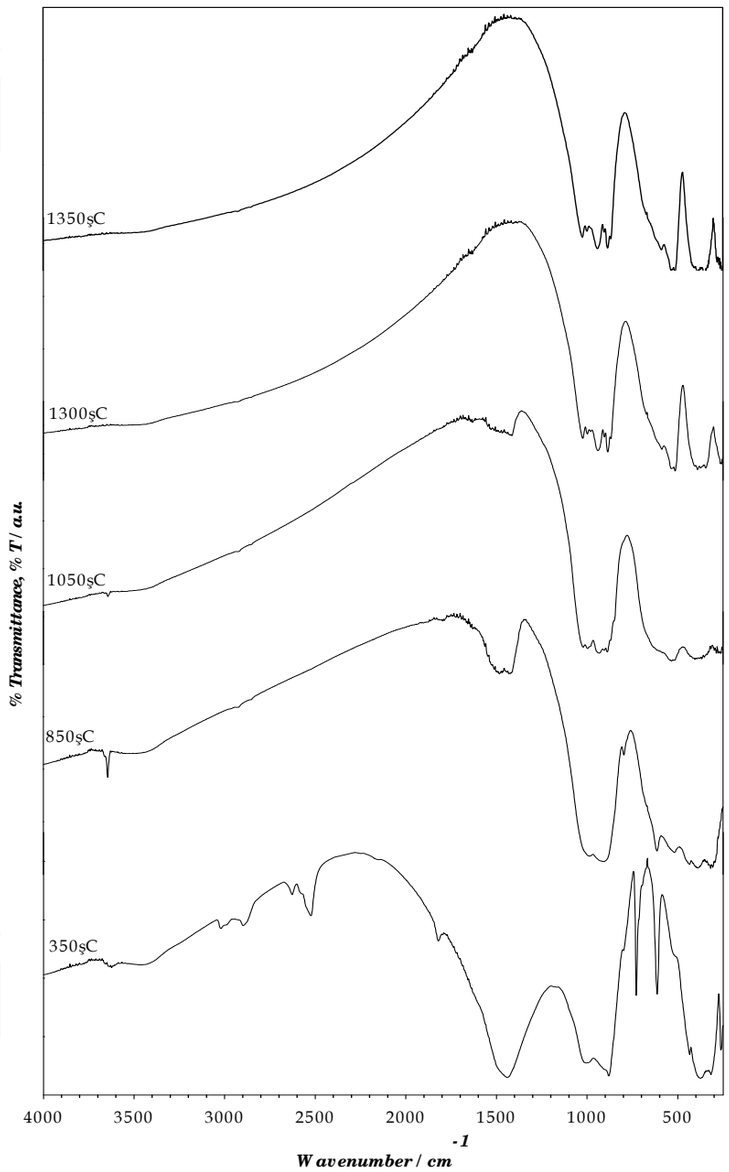

Fig. 9. Spectral FTIR patterns of D-ZS, between 350 and 1350 ºC

Up to 350ºC no significant changes are observed in the IR spectra, in comparison with the spectral patterns of the reactants. During the thermal treatment from 850ºC to 1050ºC , the bands assigned to dolomite are detected, which disappeared totally at 1300 ºC. This spectral evidence allows determining accurately the end of the decomposition of this mineral that could not be ascertained through XRD analysis.

The sharp and low intensity signal at 3643 cm^{-1}, attributed to the vibration of the bond Ca-OH, is diagnostic to identify hydrated CaO. This signal is observed over 750ºC then it weakens as temperature increases being observable until 1200ºC.
The characteristic bands of $CaZrO_3$ are detectable from 850ºC, showing enhanced definition as temperature rises up to 1350ºC, due to the increase in the formation of Ca-O-Zr bonds.
On the other hand the typical vibrations belonging to the Si-O-Si bonds of silicates are detected at 850ºC, confirming the proposed reactions. Nevertheless it is difficult to assign unambiguously this vibration to distinguish between $Ca_3Mg(SiO_4)_2$ and Ca_2SiO_4.
Despite Zr-O vibrations belonging to zircon and zirconia, absorb in a similar spectral region, due to the similar coordination and bonding; the typical ZrO_2 absorption located at 574 and 490 cm^{-1}, are present until 1300ºC.
MgO could be observable through the shoulder at 671 cm^{-1}, in the low energy region in the spectra of the specimens treated over 1200ºC.

3.3.3 Microstructure of the material D-ZS

Concerning the morphology of the material D-ZS obtained at 1350 ºC, which can be seen in Fig. 10, the formation of a bulk porous microstructure is observable, with a quite different microstructure in comparison with the D-Z specimen.
Indeed the refractory obtained from the D-ZS batch seems to be more porous and smaller in the size of the grains than the D-Z batch; and also in contrast with this material, in the case of D-ZS a very well developed three dimensional network microstructure was observed for this composite material. This feature is probably due to the liberation of CO_2, through the silicate network, that forms a homogeneous open pore structure.
The analysis of the backscattering image shows that the grains with bright contrast are belonging to the Zr-compounds; whereas those with dark contrast should be mainly attributed to MgO and Ca_2SiO_4. Moreover it is clearly observed that the grains are connected to each other via thick necks, suggesting that in this composite the Zr-phases have a "direct" bond to the other components, with good mechanical integrity. In addition the X-ray microanalysis is in fair agreement with the global composition, estimated from XRD data.

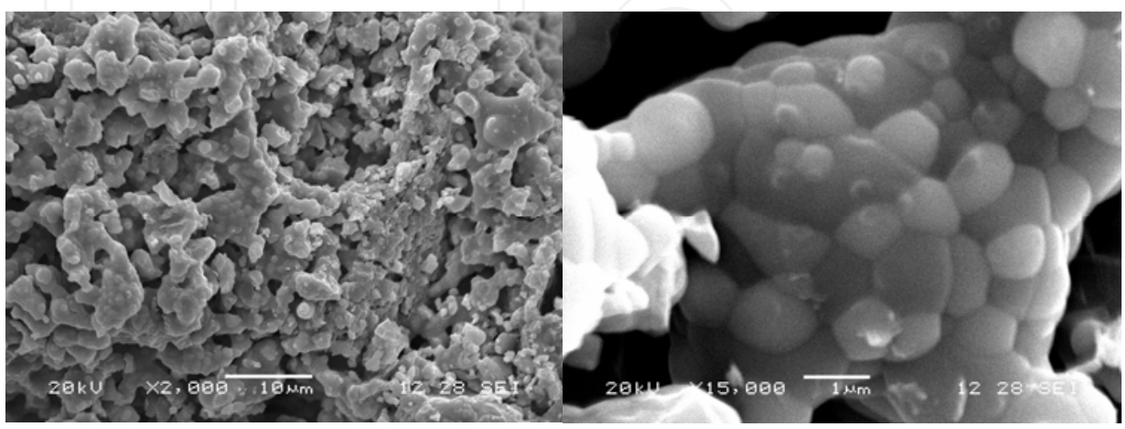

Fig. 10. SEM micrograph of D-ZS materials obtained at 1350 ºC The backscattering image is shown on the right

4. Conclusions

Dolomites from Olavarría have got mineralogical, chemical, granulometric, and specific surface characteristics that make them appropriate to obtain MgO-$CaZrO_3$ refractory materials manufacture by a simple processing at high temperature by solid-state reaction.
The process used in this study is very cost-effective because of the use of a natural ore and commercial grade zirconium sources.
The phases formed during the refractory material synthesis could be well characterized, structurally and spectroscopically, by combination of XRD and FTIR techniques.
The final composition is dependent of the Zr-sources. When ZrO_s is employed the preparation optimal temperature can be estimated at 1400ºC and the main co-products are ZrO_2(ss), the spinel $MgAl_2O_4$ and β-CS_2. When $ZrSiO_4$ is used the principal co-product is Ca_2SiO_4, accompanying by ZrO_2(ss), the spinel $MgAl_2O_4$ and the mixed oxide $Mg_2Zr_5O_{12}$, in a minor proportion. The final product is formed at 1350 ºC.
Despite the high quartz-SiO_2 content of Argentine dolostones, in comparison with the dolomitic mineralogy of other deposits in the world, the composition of phases and the microstructures achieved meet the requirements for cement kiln refractories.
The morphology of the samples shows that the Zr-phases are well dispersed within the composite matrix. In addition, in the powdered specimen obtained using zircon the "direct" bonding of the compounds could be confirmed.

5. References

Aras, A. (2004). The change of phases composition in kaolinite- and illite-rich clay-based ceramic bodies. *Appl. Clay Sci.*, Vol.24, No.3-4, (February 2004), pp.257-269, ISSN 0169-1317

Contreras, J. E.; Castillo, G.A.;Rodríguez, E.A.;Das, T.K. & Guzmán, A.M. (2005). Microstructure and properties of hercynite-magnesia-calcium zirconate refractory mixtures. *Mater. Charact.*, Vol. 54, No.4-5, (May 2005), pp. 354-359, ISSN 1044-5803

Cotton, F. A. & Wilkinson, G. (1988). Advanced Inorganic Chemistry (5Th Edition), John Wliley & Sons, ISBN 0-471-84997-9, United States of America

Dawson, P.; Hargreave M. M. & Wilkinson, G. R. (1971). The vibrational spectrum of zircon (ZrSiO4). *J Phys. C: Solid State Phys.*, Vol. 4, No.2, (February 1971), pp. 240-256, ISSN 0022-3719

De Aza, A. H.; Pena, P.; Rodríguez, M. A.; Torrecillas, R. 6 de Aza, S. (2003). New spinel-containing refractory cements. *J Eur. Ceram. Soc.*, Vol.23, No.5, (April 2003), pp. 737-744, ISSN 0955-2219

Domanski, D.; Urretavizcaya, G.; Castro, F. J. & Gennari, F. C. (2004). Mechanochemical Synthesis of Magnesium Aluminate Spinel Powder at Room Temperature. *J Am. Ceram. Soc.*, Vol. 87, No.11, (November 2004), pp. 2020-2024, ISSN 0002-7820

Gómez Peral, L. E., Poiré, D. G., Strauss, H. & Zimmermann, U., (2007). Chemostratigraphy and diagenetic constraints on Neoproterozoic carbonate successions from the Sierras Bayas Group, Tandilia System, Argentina. *Chem. Geol.* Vol.237, No.1-2, (February 2007), pp. 109–128, ISSN 0009-2541

Gou, Z.; Chang, J. & Zhai, W. (2005). Preparation and characterization of novel bioactive dicalcium silicate ceramics. *J Eur. Ceram. Soc.*, Vol.25, No.9, (June 2005), pp. 1507–1514, ISSN 0955-2219

Goto, K. & Lee, W. (1995). The "Direct Bond" in Magnesia Chromite and Magnesia Spinel Refractories. *J Am. Ceram. Soc.*, Vol. 78, No.7, (July 1995), pp. 1753-1760, ISSN 0002-7820

Khalil, N M. A.; El-Hemaly, S. A. S. & Girgis, L. G. (2001). Aluminous cements containing magnesium aluminate spinel from Egyptian dolomite. *Ceram. Int.*, Vol.27, No.8, pp. 865-873, ISSN 0272-8842

Kingery, W. D.; Bowen, H. K. & Uhlmann, D.R. (1976). *Introduction to ceramics* (2nd Edition), John Wiley & Sons, Inc., ISBN 0-471-47860-1, United States of America.

Lavat, A. E. & Grasselli, M. C. (2007). Phase evolution during preparation of spinel-containing refractory cements from argentine dolomite. *Adv. In Tech. of Mat. and Mat. Proc. J (ATM)*, Vol. 9 No. 1, pp. 103-108, ISSN 1440-0731

Lavat, A. E.; Grasselli, M. C. & Giuliodori Lovecchio, E. (2010). Effect of alpha and gamma polymorphs of alumina on the preparation of $MgAl_2O_4$ spinel-containing refractory cements. *Ceram. Int.*, Vol. 36, No.1, (January 2010), pp. 15-21, ISSN 0272-8842

Neumayer D. A. & Cartier, E. (2001). Materials characterization of ZrO_2– SiO_2 and HfO_2–SiO_2 binary oxides deposited by chemical solution deposition. *J Appl. Phys.*, Vol 90, No. 4, (August 2001), pp. 1801-1808, ISSN 0021-8979

Obregón, A.; Rodríguez-Galicia, J. L., López-Cuevas, J., Pena, P. & Baudín, C. (2011). MgO-$CaZrO_3$-based refractories for cement kilns. *J Eur. Ceram. Soc.*, Vol.31, No.1-2, (January-February 2011), pp. 61-74, ISSN 0955-2219

Orera, V. M.; Pecharromán, C.; Peña, J. I.; Merino, R. I. & Serna, C. J. (1998). Vibrational spectroscopy of $CaZrO_3$ single crystals. *J Phys.: Condens. Matter*, Vol. 10, No.3, (August 1998), pp. 7501-7510, ISSN 0953-8984

Ozel, E & Turan, S. (2007). Production of coloured zircon pigments from zircon. *J Eur. Ceram. Soc.*, Vol. 27, No.2-3, pp. 1751-1757, ISSN 0955-2219

Popa, M.; Kakihana, M.; Yoshimura, M. & Calderón-Moreno; J.M. (2006). Zircon formation from amorphous powder and melt in the silica-rich region of the alumina-silica-zirconia system. *J Non-Cryst. Solids*, Vol. 352, No.52-54, (December 2006), pp. 5663-5669, ISSN 0022-3093

Prasanth, C.S.; Padma Kumar, H.; Pazhani, R.; Solomon, S.; Thomas, J. K. (2008). Synthesis, characterization and microwave dielectric properties of nanocrystalline $CaZrO_3$ ceramics. *J Alloys Compd.*, Vol. 464, No.1-2, (September 2008), pp. 306–309, ISSN 0925-8388

Qotaibi, Z.; Diouri, A.; Boukhari, A.; Taibi, M. & Aride, J. (1998). Analysis of magnesia chrome refractories weared in a rotary cement kiln. *Ann. Chim. Sci. Mat.*, Vol.23, No.1-2, (January-February 1998), pp. 169-172, ISSN 01551-9107

Rodriguez, J. L. , De Aza, A. H.; Pena, P.; Campo, J.; Convert, P. & Turrillas, X. (2002). Study of Zircon-Dolomite monitored by neutron thermodiffractometry. *J Solid State Chem.*, Vol. 166, No.2, (July 2002), pp. 426-433, ISSN 0022-4596

Rodriguez-Galicia, J. L.; Fernández-Arguijo, B.; Rendón-Ángeles, J. C.; Pena, P.; Valle-Fuentes, J. F. & López-Cuevas, J. (2005). Reaction sintering of Mexican dolomite. *Bol. Soc. Esp. Ceram. V.*, Vol. 44 No.4, (July-August 2005), pp. 245-250, ISSN 0366-3175

Rodriguez-Galicia, J.L.; De Aza, A.H.; Rendón-Ángeles, J.C. & Pena, P. (2007). The mechanism of corrosion of MgO-$CaZrO_3$-calcium silicate materials by cement clinker. *J Eur. Ceram. Soc.*, Vol. 27, No1, pp. 79-89, ISSN 0955-2219

Serena, S.; Sainz, M.A. & Caballero, A. (2004). Corrosion behavior of MgO/$CaZrO_3$ refractory matrix by clinker. *J Eur. Ceram. Soc.*, Vol. 24, No.8, (July 2004), pp. 2399-2406, ISSN 0955-2219

Serena, S.; Sainz, M.A. & Caballero, A. (2005). Thermodynamic assessment of the system ZrO_2-CaO-MgO using new experimental results Calculation of the isoplethal section MgO.CaO-ZrO_2. *J Eur. Ceram. Soc.*, Vol. 25, No.5, (February 2005), pp. 681-693, ISSN 0955-2219

Singh, R. K. & Upadhyaya, K. S. (1972). Crystal dynamics of magnesium oxide. *Phys. Rev. B*, Vol. 6, No. 4, (August 1972), pp. 1589-1596, ISSN 1098-0121

Suzuki, Y.; Morgan, P.E.D & Ohji, T. (2000). New uniformly porous $CaZrO_3$/MgO composites with three- dimensional network structure from natural dolomite. *J Am. Ceram. Soc.*, Vol. 83, No. 8, (August 2000), pp. 2091-2093, ISSN 0002-7820

Wilson, M. J. (1987). A handbook of determinative methods in clay mineralogy. Blackie & Son Ltd. Place, ISBN 0-412-00901-3

Zoz, E. I. & Karaulov, A. G. (1991). Comparative study of the solid solutions in the ZrO_2-HfO_2-MgO(CaO) systems. *Refract. Ind. Ceram.*, Vol. 32, No.3 (March 1991), pp. 109-112, ISSN 0034-3102

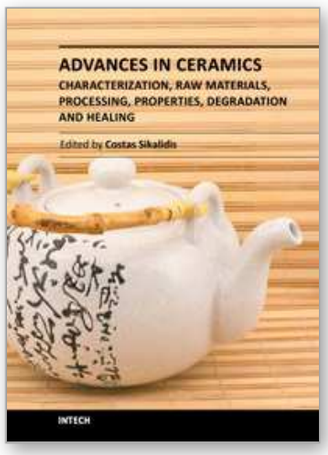

Advances in Ceramics - Characterization, Raw Materials, Processing, Properties, Degradation and Healing
Edited by Prof. Costas Sikalidis

ISBN 978-953-307-504-4
Hard cover, 370 pages
Publisher InTech
Published online 01, August, 2011
Published in print edition August, 2011

The current book consists of eighteen chapters divided into three sections. Section I includes nine topics in characterization techniques and evaluation of advanced ceramics dealing with newly developed photothermal, ultrasonic and ion spattering techniques, the neutron irradiation and the properties of ceramics, the existence of a polytypic multi-structured boron carbide, the oxygen isotope exchange between gases and nanoscale oxides and the evaluation of perovskite structures ceramics for sensors and ultrasonic applications. Section II includes six topics in raw materials, processes and mechanical and other properties of conventional and advanced ceramic materials, dealing with the evaluation of local raw materials and various types and forms of wastes for ceramics production, the effect of production parameters on ceramic properties, the evaluation of dental ceramics through application parameters and the reinforcement of ceramics by fibers. Section III, includes three topics in degradation, aging and healing of ceramic materials, dealing with the effect of granite waste addition on artificial and natural degradation bricks, the effect of aging, micro-voids, and self-healing on mechanical properties of glass ceramics and the crack-healing ability of structural ceramics.

How to reference
In order to correctly reference this scholarly work, feel free to copy and paste the following:

Araceli Lavat, Marîa Cristina Grasselli and Eugenia Giuliodori Lovecchio (2011). Characterization of the Firing Steps and Phases Formed in Mg-Zr-Containing Refractory Dolomitic Materials, Advances in Ceramics - Characterization, Raw Materials, Processing, Properties, Degradation and Healing, Prof. Costas Sikalidis (Ed.), ISBN: 978-953-307-504-4, InTech, Available from: http://www.intechopen.com/books/advances-in-ceramics-characterization-raw-materials-processing-properties-degradation-and-healing/characterization-of-the-firing-steps-and-phases-formed-in-mg-zr-containing-refractory-dolomitic-mate

INTECH
open science | open minds

InTech Europe
University Campus STeP Ri
Slavka Krautzeka 83/A
51000 Rijeka, Croatia
Phone: +385 (51) 770 447
Fax: +385 (51) 686 166
www.intechopen.com

InTech China
Unit 405, Office Block, Hotel Equatorial Shanghai
No.65, Yan An Road (West), Shanghai, 200040, China
中国上海市延安西路65号上海国际贵都大饭店办公楼405单元
Phone: +86-21-62489820
Fax: +86-21-62489821

IntechOpen